0 0 0 0 4 9 0 5 7 0 4

Submitted to Physical Review B
(Solid State)

RECEIVED
LAWRENCE
BERKELEY LABORATORY

MAR 8 1978

LIBRARY AND
DOCUMENTS SECTION

UC-4

LBL-6996
Preprint

THE TEMPERATURE-DEPENDENT SURFACE STRUCTURE, COMPOSITION AND ELECTRONIC PROPERTIES OF THE CLEAN $SrTiO_3$(111) CRYSTAL FACE: LEED, AES, ELS AND UPS STUDIES

Wei Jen Lo and G. A. Somorjai

December 16, 1977

Prepared for the U. S. Department of Energy
under Contract W-7405-ENG-48

For Reference

Not to be taken from this room

LBL-6996

LEGAL NOTICE

This report was prepared as an account of work sponsored by the United States Government. Neither the United States nor the Department of Energy, nor any of their employees, nor any of their contractors, subcontractors, or their employees, makes any warranty, express or implied, or assumes any legal liability or responsibility for the accuracy, completeness or usefulness of any information, apparatus, product or process disclosed, or represents that its use would not infringe privately owned rights.

0 0 0 0 4 9 0 3 7 0 5

The Temperature-Dependent Surface Structure, Composition and Electronic Properties of the Clean $SrTiO_3$(111) Crystal Face: LEED, AES, ELS and UPS Studies.

by

Wei Jen Lo* and G. A. Somorjai

Materials and Molecular Research Division, Lawrence Berkeley Laboratory, and Department of Chemistry, University of California, Berkeley, California, 94720, U.S.A.

* also associated with:

Department of Physics, University of California, Berkeley, CA 94720, U.S.A.

0 0 0 0 4 9 0 0 7 0 6

ABSTRACT

Low-energy electron diffraction (LEED), Auger electron spectroscopy (AES), electron energy loss (ELS) and ultraviolet photoelectron spectroscopies (UPS) were used to study the structure, composition, and electron energy distribution of clean single crystal (111) face of strontium titanate (perovskite). The dependence of the surface chemical composition on the temperature has been observed along with corresponding changes in the surface electronic properties. High-temperature Ar ion bombardment causes an irreversible change in the surface structure, stoichiometry and electron energy distribution. In contrast to the TiO_2 surface, there are always significant concentration of Ti^{3+} in an annealed ordered $SrTiO_3$(111) surface. This stable active Ti^{3+} monolayer on top of a substrate with large surface dipole potential makes $SrTiO_3$ superior to TiO_2 when used as a photo anode in the photoelectrochemical cell.

Introduction

Strontium titanate $SrTiO_3$ is one of the few stable materials that can decompose water into hydrogen and oxygen with the assistance of light of band gap energy (3.2 eV at 25°C) or greater in the photoelectrochemical cell (1). The photoelectrolysis can be sustained using $SrTiO_3$ as an anode (where oxygen evolves) and platinum as a cathode (hydrogen evolution), without the use of external potential. This may be contrasted with the TiO_2 photoanode (2) that requires +0.2 volt external potential to carry out the same photoassisted water dissociation reaction in the same experimental configuration.

In addition to possessing this remarkable photocatalytic property, strontium titanate has interesting semiconducting, superconducting, and optical properties. Stoichiometric $SrTiO_3$ is an insulator transparent to visible light. At room temperature, it is cubic but undergoes a transition to a tetragonal structure at about 110K (3). When strontium titanate is reduced, it takes on a blue color and becomes semiconducting. Strontium titanate displays a number of interesting photochromic and electrochromic properties (4) when doped with metal ions and hence has potentially important electro-optic applications in areas such as image storage, photochromism, and electrochromism. Doped strontium titanate is also a superconductor (5) with a transition temperature of about 0.3K. The atomic structure and electronic properties of bulk strontium titanate crystal have been thoroughly studied both by theory and by experiments. Theoretical calculations of the bulk band structure of $SrTiO_3$ have been reported by Kahn, et al.(6) and Matheiss (7) and are in fairly good agreement with the results of photoemission experiments by Shirley, et al.(8).

Compared to the data that have been accumulated on the bulk properties, the surface structure and electron energy distribution of the $SrTiO_3$ surface are relatively unexplored. Walfram, et al.(9) have carried out theoretical surface energy hand calculation of strontium titanate which suggests the existence of a highly localized d-electron surface band in the band-gap region and emphasizes its importance in surface chemical reactions. Experiments (10,11) have been performed only recently that investigate the $SrTiO_3$ surface electron distribution, using ultraviolet photoelectron spectroscopy (UPS).

Since the catalytic properties of surfaces depends strongly on their atomic surface structure, chemical compositon and electronic distribution, it is important to investigate all of these properties. In this report, a combination of surface analysis techniques has been employed to characterize the clean strontium titanate single crystal face with (111) orientation. Low-energy electron diffraction (LEED) and Auger electron spectroscopy (AES) were used to study the surface structure and chemical composition, respectively. Electron energy distributions were studied by energy loss spectroscopy (ELS) and ultraviolet photoemission spectroscopy (UPS). It is found that for $SrTiO_3$, the crystal temperature plays an important role in determining its surface structure, chemical composition and electronic distribution. By comparing the surface properties of TiO_2 and $SrTiO_3$, we attempt to explain the difference in the photoactivity observed when these materials were utilized in the photoelectrochemical cell.

Experimental

All the experiments were performed in a stainless-steel ultra-high vacuum (UHV) chamber evacuated by ion and water-cooled titanium sublimation pumps. The base pressure during these experiments was in the low 10^{-10} Torr range.

A double pass cylindrical mirror analyzer (CMA) with a coaxial electron gun was used as the primary electron source and electron energy analyzer by which electrons emitted into a conical segment with half angle of 42.3° from the axis of the analyzer were collected. In all Auger electron analysis, the CMA was operated at a constant resolution of 1.5 eV. In this way we could resolve detail structures of the peaks in the $\frac{dN}{dE}$ Auger spectra, and give reliable estimates of strontium to oxygen and oxygen to titanium ratios under different conditions of surface preparation.

A primary electron beam with energies between 60-180 eV was used in the electron energy loss experiments. The electron energy loss spectra (ELS) were obtained either by directly measuring the electron energy distribution N(E) as a function of energy loss or its second derivative $-\frac{d^2N}{dE^2}$. Both methods yielded the same loss peaks except the features in the ELS $-\frac{d^2N}{dE^2}$ spectra were enhanced. The CMA was operated in the retarded mode with pass energy at 50 eV. However, since the primary electron beam was not energy analyzed, the ultimate resolution was limited by the thermal energy spread of the incident electrons which was about 0.5 eV. The energy positions of the loss peaks were independent of incident electron energies in the range of 60-180 eV. All energy loss spectra reported in this paper were obtained with incident energies ~100 eV, whose features were very surface-sensitive.

In the UPS studies, the cold cathode discharge lamp was operated to generate the HeI spectral line at 21.2 eV. A self-made two-stage differential pumping manifold was employed to minimize the helium leak flow from the discharge lamp into the ultrahigh vacuum chamber which maintained a pressure of $1\text{-}2\times10^{-9}$ Torr during all UPS experiments. The mass spectrometer indicated that the pressure raise was due to the increase of helium partial pressure in the chamber. The specimen was positioned with its surface normal coincident with the axis of CMA. The angle of incidence of the photons on the specimen was 75° from the normal. The analysis was operated with a constant resolution of 0.35 eV. Typically a spectrum could be obtained within 5 minutes.

The specimen used was a 99.99% undoped strontium titanate single crystal with perouskite structure. Samples of (111) orientation, as determined by the Laue back reflection technique, were cut from this crystal and mechanically polished using 0.05 μm Al_2O_3 powders. The specimen was then rinsed in distilled water and mounted on a high density alumina holder, which had a tungsten heater wire located at the back of the sample to facilitate the radiation heating of the crystal. A LEED optics made by Physical Electronics was used to study the surface structure after annealing. Two samples of (111) orientation have been prepared and both gave essentially the same results.

For argon ion bombardment of strontium titanate surface, the vacuum chamber was back-filled with argon to a pressure of 6×10^{-5} Torr. With an accelerating voltage of 2 KeV, the ion bombardment could typically deliver an argon ion beam of 20 μA to the sample surface.

Results

1) LEED and AES Studies of the Surface Structure and Chemical Composition of Clean $SrTiO_3(111)$ Surface as a Function of Temperature.

The LEED pattern obtained from the $SrTiO_3(111)$ surface at room temperature is shown in Fig.1. The surface exhibits a stable (1×1) surface structure after Ar ion bombardment at 27°C to remove impurities then annealing at 600°C for 30 mins. However, after Ar ion bombarding at 600°C, the surface seems to facet as indicated by the LEED pattern (Fig. 2), and the surface assumes a complex structure. The (1×1) surface structure can be restored after removal of the faceted surface by extended Ar ion bombardment (20 mins) at 27°C followed by annealing at 600°C for 20 mins.

The Auger electron spectrum for the clean $SrTiO_3(111)$-(1×1) surface at 27°C is shown in Fig. 3. The value of the Auger peak-to-peak ratios of $\frac{Sr(65eV)}{O(510eV)}$ and $\frac{O(510eV)}{Ti(380eV)}$ in the AES spectrum for this surface are 1.5 and 2.0, respectively. Figure 4 shows the AES spectrum from the $SrTiO_3(111)$ surface at a temperature of 600°C. By comparing with the AES spectrum in Fig. 3 we find the shape of titanium Auger peak at 416 eV has changed and the Auger $\frac{Sr(65eV)}{O(510eV)}$ ratio drops to 1.1. The emission from the hot filament of the heater prevented LEED observation of $SrTiO_3(111)$ surface at 600°C. After cooling the crystal to 27°C, the AES spectrum returned to that shown in Fig. 3 and LEED showed a (1×1) surface structure at 27°C. This heating and cooling cycle has been repeated several times and the above results are quite reproducible. It appears that the surface concentration of strontium becomes less with increasing temperature in a reversible manner.

Figure 5 shows the AES spectrum of the clean $SrTiO_3(111)$ surface after Ar ion bombardment at 27°C. The detailed feature of the Auger titanium

and oxygen peaks in this AES spectrum are very similar to those of Ar ion sputtered TiO_2 surface (12). While there is only little change in the value of the Auger $\frac{O(510eV)}{Ti(380eV)}$ ratio, upon ion bombardment, the $\frac{Sr(65eV)}{O(510eV)}$ peak ratio shows a remarkable increase from 1.5 (for (1×1) surface) to 2.8 (for Ar ion bombarded surface at 27°C). It appears that Ar ion bombardment at 27°C removes oxygen preferentially from the surface region.

The AES spectra of the $SrTiO_3$(111) surfaces which were Ar ion bombarded at 27°C and 600°C, respectively, are shown in Fig. 6. Both spectra were taken at 27°C after the same 2 keV Ar ion dosage to the surface. Comparison of these spectra exhibits two distinct differences. First, we find that the shapes of titanium Auger peaks in the AES spectra are different. For the room temperature ion bombarded $SrTiO_3$ surface, the shape of the Auger titanium peak at 416 eV resembles that of the same peak in the Ar ion sputtered TiO_2 surface. The shape of the corresponding titanium peak for the $SrTiO_3$ surface after Ar ion sputtering at 600°C resembles to that of the same peak in the well-annealed TiO_2 surface. Second, the value of the Auger $\frac{Sr(65eV)}{O(510eV)}$ ratio is higher for the $SrTiO_3$ surface after high-temperature (600°C) ion sputtering. It increases from 2.8 (for ion sputtering at 27°C) to 4.1 (for ion sputtering at 600°C). It appears that high-temperature argon ion-bombardment induces a large enrichment of strontium in the $SrTiO_3$ surface.

2) ELS and UPS Studies of Electron Energy Distribution at the clean $SrTiO_3$(111) Surface as a Function of Temperature.

a) Electron energy loss spectroscopy. The energy loss spectra for the clean $SrTiO_3$(111) crystal faces obtained after the different surface treatments are shown in Fig. 7. In Fig. 7(a) the ELS spectrum of the clean $SrTiO_3$ surface

is shown after Ar ion bombardment at 27°C. There are six distinct transitions at 13.1, 10.3, 7.7, 5.6, 3.1 and 1.6 eV. The gross features of this spectrum are very similar to those reported for the Ar ion sputtered TiO_2 (12) surfaces, except on the $SrTiO_3$ surface there is one more transition at 7.7 eV. Both TiO_2 and $SrTiO_3$ surfaces show a distinct 1.6 eV transition after Ar ion sputtering at 27°C that is associated with the presence of Ti^{3+} ions at the surface (13-14). The ELS spectrum obtained at 300°C upon annealing the crystal at this temperature is shown in Fig. 7(b). The intensity of 10.3 eV transition has increased while the intensity of 7.7 eV has decreased. There is also an observable reduction in the intensity of the 1.6 eV transition. Figures 7(d) and 7(d) show the ELS spectra for the same $SrTiO_3$ crystal surface at 500°C and 600°C, respectively. We find that there is a continuous reduction of the intensity of the 1.6 eV transition that is associated with the presence of Ti^{3+} and it finally disappears at 600°C. After cooling the crystal back to 300°C, the 1.6 eV transition reappears as shown in Fig. 7(e). Successive cooling the crystal back to room temperature, results in an ELS spectrum shown in Fig. 7(f). In comparison with that in Fig. 7(e), the intensity of 1.6 eV transition in Fig. 7(f) is enhanced. The LEED patterns from the surface that yield the ELS spectrum of Fig. 7(f) indicates the presence of an ordered (1×1) surface sturcture. The heating and cooling cycles havebeen repeated several times and the results are very reproducible. Thus, it appears that the composition and electronic energy distribution of the $SrTiO_3$ surface changes reversibly with surface temperature.

In Fig. 8, we show the ELS spectra for the $SrTiO_3$ surfaces that were Ar ion bombarded at 27°C and 600°C, respectively. Both surfaces have the same Ar ion dosages and the spectra were obtained when the crystal reached

room temperature after sputting. Although the relative peak intensities of the 13.1, 10.3, 5.6 and 3.1 eV transitions are similar in the two ELS spectra, the intensity of the 7.7 eV transition is higher in Fig. 8(b). In addition, while there is a distinct 1.6 eV transition in the ELS spectrum for the $SrTiO_3$ surface after Ar ion bombardment at 27°C, this transition completely disappears from the ELS spectrum for the $SrTiO_3$ surface after high-temperature (600°C) Ar ion sputtering.

b) Ultraviolet photoelectron spectroscopy. The UPS spectrum for the Ar ion sputtered surface at 27°C is shown in Fig. 9. In agreement with the work of Henrich (11), an emission at -0.6 eV below the Fermi level E_F in the band gap region is observed. This is consistent with the result obtained for Ar ion bombarded TiO_2 surfaces (12-13), which show the same -0.6 emission in the UPS spectra. This emission is associated with the presence of Ti^{3+} in the oxide surfaces (13-14). In Fig. 9, there are also other emission peaks with energies at -2.6 eV, -6.0 eV and -10.8 eV, respectively. The work function ϕ of this surface is 3.4 eV.

Subsequent annealing at 600°C resulted in the disappearance of the -10.8 eV and -2.6 eV emissions and splitting of the broad -6.0 eV peak into two emissions with energies at -6.9 eV and -4.8 eV, respectively, as shown in Fig. 10. We also find that the intensity of the -0.6 eV emission in the band gap region has been reduced. However, this emission always has a detectable intensity at 27°C, even after annealing the crystal at 800°C for two hours. The LEED pattern which corresponds to the UPS spectrum shown in Fig. 10 indicates that the surface has a (1×1) structure. The work function of this clean ordered $SrTiO_3$(111)-(1×1) surface is 5.2 eV.

The temperature dependent changes in the UPS spectra for the clean, ordered $SrTiO_3(111)$ surfaces are shown in Fig. 11 that displays the curves taken at 27°C, 300°C and 600°C. There is a continuous reduction in the intensity of the -0.6 eV emission with increasing crystal temperature. This change is reversible, after cooling the $SrTiO_3$ crystal to room temperature, the same intial UPS spectrum is obtained.

Figure 12 shows the UPS spectrum from the clean $SrTiO_3(111)$ surface after Ar ion bombardment at 600°C. This spectrum was taken at a crystal temperature of 27°C after the high-temperature sputtering process. In contrast to the room temperature Ar ion-bombarded $SrTiO_3$ surface, we find the Fermi-edge emission at -0.6 eV has disappeared almost completely. The work function of this surface is 4.0 eV.

Discussion

The change in the strontium to oxygen Auger peak ratio and the constancy of the oxygen to titanium ratio indicate oxygen and titanium are removed preferentially from the $SrTiO_3$(111) surface by Ar ion sputtering at room temperature. On annealing this sputtered surface, strontium diffuses into the bulk, thereby decreasing the strontium concentration of the surface. The chemical composition of the $SrTiO_3$(111) surface can be varied reversibly by changing the crystal temperature, as shown by AES. Although similar temperature dependent surface composition has been observed for binary alloy surfaces (15), our result is the first report of this effect for a ternary oxide compound.

Auger electron spectroscopy analysis also shows that the crystal temperature during Ar-ion sputtering can cause marked changes in the chemical composition of the $SrTiO_3$(111) surface. After a high-temperature (600°C) Ar ion sputtering treatment, there is a remarkable increase in the strontium concentration and annealing does not alter this surface composition any more. The room temperature Ar ion bombarded $SrTiO_3$ surface has a lower strontium surface concentration and its value is decreased after annealing at 600°C. This indicates that high-temperature Ar ion bombardment yields a stable Sr-rich phase on the $SrTiO_3$(111) surface, which behaves differently from the room temperature Ar ion sputtered $SrTiO_3$ surface. LEED studies also indicate structural differences between the two surfaces that were ion bombarded at 27°C and 600°C, respectively, after annealing.

The electron energy distributions of the $SrTiO_3$(111) surface as a function surface treatments are studied by ELS and UPS. The transition peaks at 13.1, 10.3, 7.7 and 5.5 eV in the ELS spectra have also been observed by

M. Cordova (16) using the ultraviolet reflectance technique. The bulk states which are involved in these transitions have been assigned (16). The ultraviolet photoemitted electrons from the $SrTiO_3$ surface come from two sources: from the states in the valence band and from states in the band gap region. While AES shows oxygen loss from the $SrTiO_3$ surface as a result of argon ion sputtering at 27°C, the ELS spectrum of the Ar ion sputtered $SrTiO_3$ surfaces shows a strong peak at 1.6 eV. Since the band gap of $SrTiO_3$ is 3.2 eV, the initial states of the 1.6 eV transition must be located in the band gap region. Indeed a band gap emission at -0.6 eV in the UPS spectrum was found in this sputtered $SrTiO_3$ surface and was assigned to be the initial states for the 1.6 eV transition. In agreement with the results for the TiO_2 surfaces (12-14), these 1.6 eV transition and -0.6 eV emission are characteristic of the presence of surface Ti^{3+} species. In contrast to the case of the TiO_2 surface, where annealing caused the complete disappearance of Ti^{3+} species, the $SrTiO_3$(111)-(1×1) ordered surface after annealing always has detectable amounts of Ti^{3+} present at room temperature. The UPS spectrum of $SrTiO_3$(111)-(1×1) shows that the width of the valence band is 6.5 eV and two major emission peaks separated by 2.1 eV are resolved. This result is consistent with the recent XPS studies of Shirley et al.(8), and gives a reasonable fit to the density of states calculations of Mattheiss (7). The difference in the shapes of valence bands in the UPS spectra between the room temperature Ar ion sputtered $SrTiO_3$ surface and the $SrTiO_3$(111)-(1×1) surface is due to the change in surface stoichiometry that is induced by Ar ion sputtering. In addition, the UPS spectrum of the $SrTiO_3$ surface after Ar ion sputtering at 27°C shows the presence of occupied states with energies around -2.6 eV which are located

right above the valence band maximum. The absence of these states on the $SrTiO_3(111)$-(1×1) surface after annealing indicates that they are extrinsic surface states induced by Ar ion sputtering at 27°C.

The reversible variation of the intensity of the -0.6 eV UPS emission and 1.6 eV ELS transition of $SrTiO_3$ surface as a function of temperature reveals that the concentration of surface Ti^{3+} species depends on the crystal temperature. At 27°C, there is a large concentration of Ti^{3+} species ($\sim 10^{14}/cm^2$) on the ordered surface. Raising the crystal temperature to 300°C, the reduction of Ti^{3+} concentration is observed and a complete disappearance of Ti^{3+} species is obtained by heating the crystal above 600°C. However, subsequent cooling of the crystal to room temperature results in the reappearance of the surface Ti^{3+} species. The combination of our ELS, UPS and AES studies indicates that the temperature of the ternary oxide crystal controls its surface stoichiometry which in turn determines many of the surface electronic properties. The persistent difference in the surface Ti^{3+} species concentration between the TiO_2 and $SrTiO_3$ surfaces at room temperature indicates that excess Sr stabilizes the formation of Ti^{3+}.

The combination of ELS, UPS, AES and LEED studies indicates that high-temperature (600°C) Ar ion sputtering treatment causes an irreversible change in the surface structure, surface chemical composition and electronic properties and yields a stable strontium-rich phase.

The different surface treatments of the $SrTiO_3$ surface result in drastic change of the work function and hence a large change in the surface dipole potential. In photo-assisted reactions on the semiconductor surface where the transport of photogenerated charge carriers at the surface is the rate-determining step, it is desirable to increase the electric field near the

surface to allow a rapid charge transfer to and from the surface. In the case of TiO_2, Ar ion sputtering produces a large concentration of Ti^{3+} species and a marked decrease in the surface dipole potential. Subsequent annealing increases the work function and the associated surface dipole potential, but removes all the Ti^{3+} species on the surface. However, in the case of $SrTiO_3$ surface where annealing also causes the increase of the work function, Ti^{3+} ions are always present at room temperature after annealing. Since the presence of surface Ti^{3+} species aids the dissociation of adsorbed water (13), an active Ti^{3+} monolayer on top of a substrate with large surface dipole potential provides a suitable catalyst for this photo-assisted reaction. The important differences in surface composition and work function shown in Fig. 13 appear to be the cause of the differences in photo-activity between TiO_2 and $SrTiO_3$ that are used in the photo-electrochemical cell (1-2).

Conclusion

Using LEED, AES, ELS and UPS we have characterized the surface structure composition and electronic distribution of the (111) single crystal surface of $SrTiO_3$. The dependence of the surface chemical composition on the temperature has been observed along with corresponding changes in the surface electronic properties. High temperature Ar ion bombardment causes an irreversible change in the surface structure, stoichiometry and associated electron energy distribution. In contrast to the TiO_2 surface, there are always significant concentration of Ti^{3+} species on the $SrTiO_3$ surface which also has a larger surface dipole potential. The stable, active Ti^{3+} monolayer on top of a substrate with large surface dipole potential makes $SrTiO_3$ superior to TiO_2 when used as a photoanode in the photoelectrochemical cell.

Acknowledgment:

We are grateful to V. E. Henrich for communicating his results to us prior to publication of his work. This work was supported by the Division of Basic Energy Sciences, United States Department of Energy.

References

1. a) M. S. Wrighton, A. B. Ellis, P. T. Wolczanski, D. L. Morse, H. G. Abrahamson and D. S. Grinley, J. of Amer. Chem. Soc. 98, 2774 (1976).

   b) M. S. Wrighton, P. T. Wolczanski and A. B. Ellis, J. of Solid State Chem. 22, 17 (1977).

2. M. S. Wrighton, D. S. Gimley, P. T. Solczanski, A. B. Ellis, D. L. Morse and A. Linz, Proc. Nat. Acad. Sci., U.S.A. 72, 1518 (1975).

3. Y. T. Sihvonen, J. Appl. Phys. 38, (1967) 4431.

4. B. Faughman, Phys. Rev. B 4, 3623 (1971).

5. J. F. Schooley, W. R. Hosler, E. Ambler, J. H. Becker, M. L. Cohen and O. S. Koonce, Phys. Rev. Letts. 14, 305 (1965).

6. A. H. Kahn and A. J. Leyendecker, Phys. Rev. 135, A1321 (1964).

7. L. F. Mattheiss, Phys. Rev. B6, 4718 (1972).

8. S. P. Kowalczyk, F. R. McFeely, L. Ley, V. T. Gritsyna, and D. A. Shirley, Solid State Comm. 23, 161 (1977).

9. T. Wolfram and F. J. Morin, Appl. Phys. 8, 125 (1975).

10. R. A. Powell and W. E. Spicer, Phys. Rev. B13, 2601 (1976).

11. J. G. Mavroides, V. E. Henrich, H. J. Zeiger, G. Dresselhaus, J. A. Kafalas and D. F. Kolesar, J. Electrochem. Soc., to be published.

12. Y. W. Chung, W. J. Lo and G. A. Somorjai, Surf. Sci. 64, 588 (1977).

13. W. J. Lo, Y. W. Chung and G. A. Somorjai, Surf. Sci., to be published.

14. V. E. Henrich, G. Dresselhaus and H. J. Zeiger, Phys. Rev. Letts. 36, 1335 (1976).

15. Steven H. Overbury, Ph.D. thesis, Department of Chemistry, University of California, Berkeley, 1976.

16. M. Cardona, Phys. Rev. 140, A651 (1965).

Fig. 1. Low-energy electron diffraction patterns of the clean $SrTiO_3(111)$ surface after Ar ion bombardment at 27°C and subsequent annealing at 600°C. (a) E_p = 24 eV. (b) E_p = 32 eV.

Fig. 2. Low-energy electron diffraction patterns of the clean $SrTiO_3(111)$ surface after Ar ion bombardment at 600°C and subsequent annealing at 600°C. (a) E_p = 25 eV. (b) E_p = 34 eV.

Fig. 3. Auger electron spectrum of the clean ordered $SrTiO_3(111)$-(1×1) surface at 27°C.

Fig. 4. Auger electron spectrum of the clean ordered $SrTiO_3(111)$ surface at a temperature of 600°C.

Fig. 5. Auger electron spectrum of the clean room temperature argon ion bombarded $SrTiO_3$ surface. The AES spectrum taken at 27°C.

Fig. 6. AES spectra of:
(a) room temperature, (b) high temperature (600°C)
Ar ion bombarded $SrTiO_3$ surfaces. Both spectra were taken at room temperature.

Fig. 7. Electron energy loss spectra of the clean $SrTiO_3(111)$ surface at temperatures of (a) 27°C, (b) 300°C, (c) 500°C, (d) 600°C, (e) 300°C, (f) 27°C after room temperature Ar ion bombardment. The LEED pattern from the surface that corresponds to (f) indicates an ordered (1×1) surface structure.

Fig. 8. Electron energy loss spectra of the clean $SrTiO_3(111)$ surfaces (a) after room temperature Ar ion bombardment, (b) after high temperature (600°C) Ar ion bombardment. Both spectra were taken at room temperature of 27°C.

Fig., cont'd.

Fig. cont'd.

Fig. 9. The UPS spectrum of the Ar ion bombarded clean $SrTiO_3$ surface at 27°C.

Fig. 10. The UPS spectrum of the clean, ordered $SrTiO_3$(111)-(1×1) surface. The spectrum was taken at a temperature of 27°C.

Fig. 11. The UPS spectra of the clean, ordered $SrTiO_3$(111) surfaces taken at temperatures of 27°C, 300°C and 600°C, respectively.

Fig. 12. The UPS spectrum of the high-temperature (600°C) Ar ion sputtered $SrTiO_3$(111) surface. The spectrum was taken at 27°C.

Fig. 13. The electron energy loss spectra and the corresponding work functions of: (a) clean, ordered $SrTiO_3$(111)-(1×1) surface, (b) ordered TiO_2(100)-(1×3) surface, and the (c) clean Ar ion sputtered TiO_2 surface. Notice the persistent appearance of 1.6 eV transition on the $SrTiO_3$(111)-(1 1) surface which has also a larger work function than that of the Ar sputtered TiO_2 surface. All ELS spectra were taken at room temperature.

A

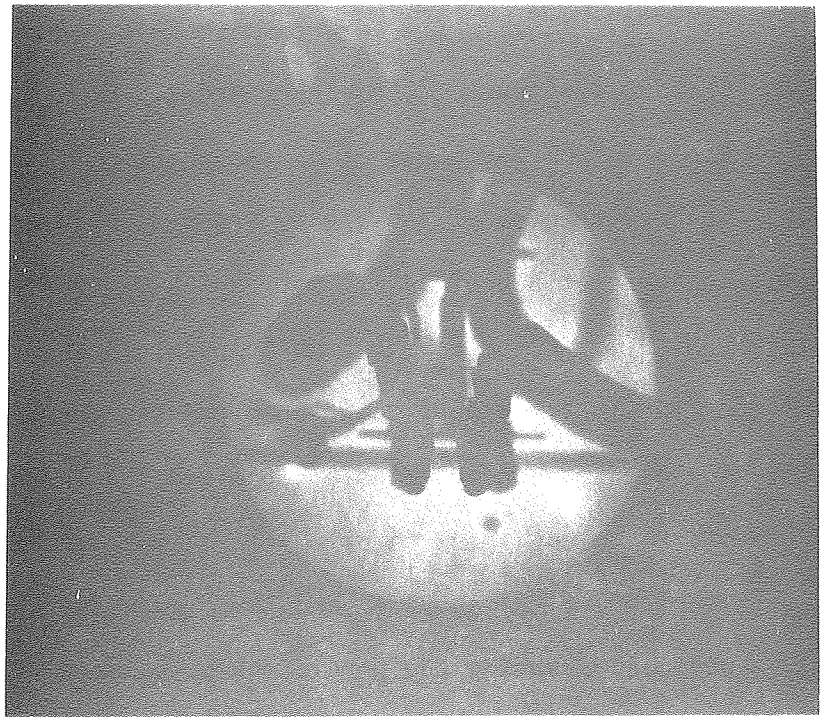

B

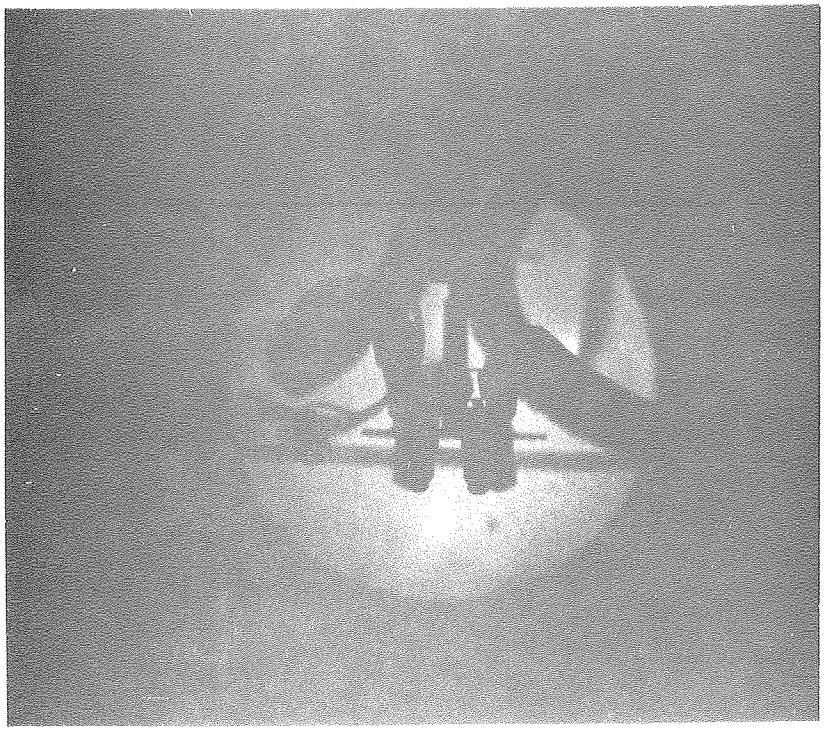

Fig. 1

XBB 770-12422

A

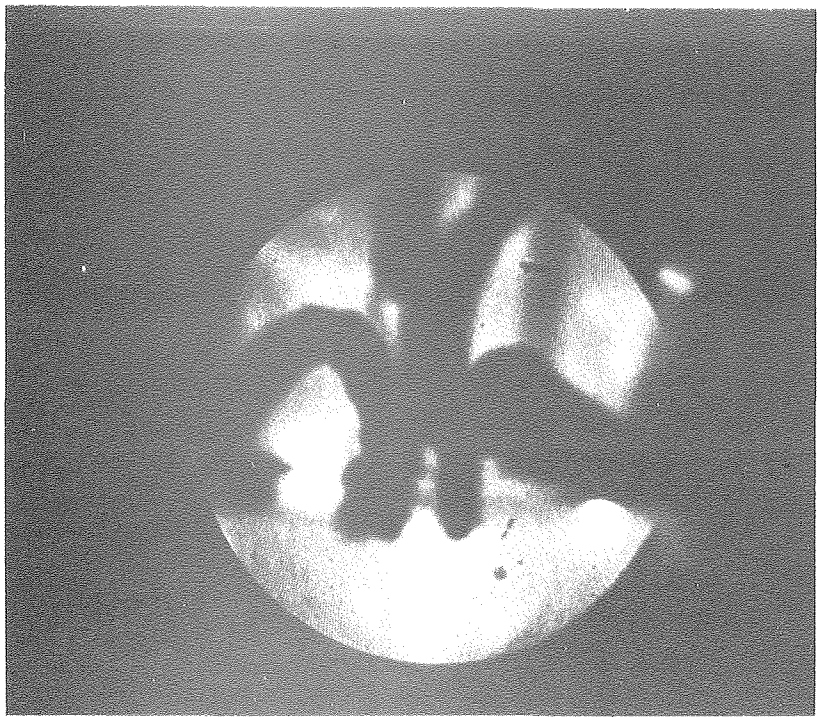

B

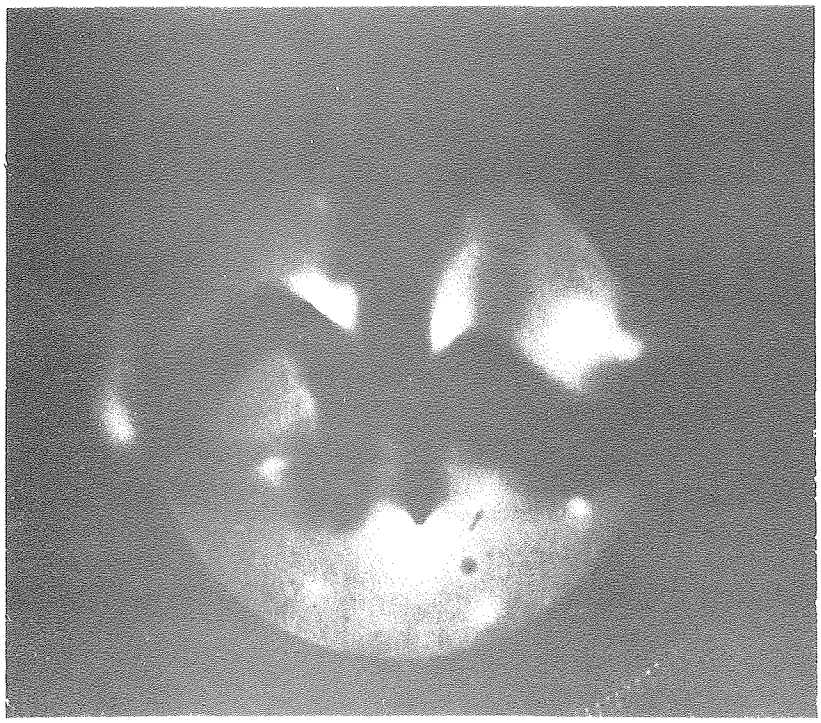

Fig. 2a,b

XBB 770-12423

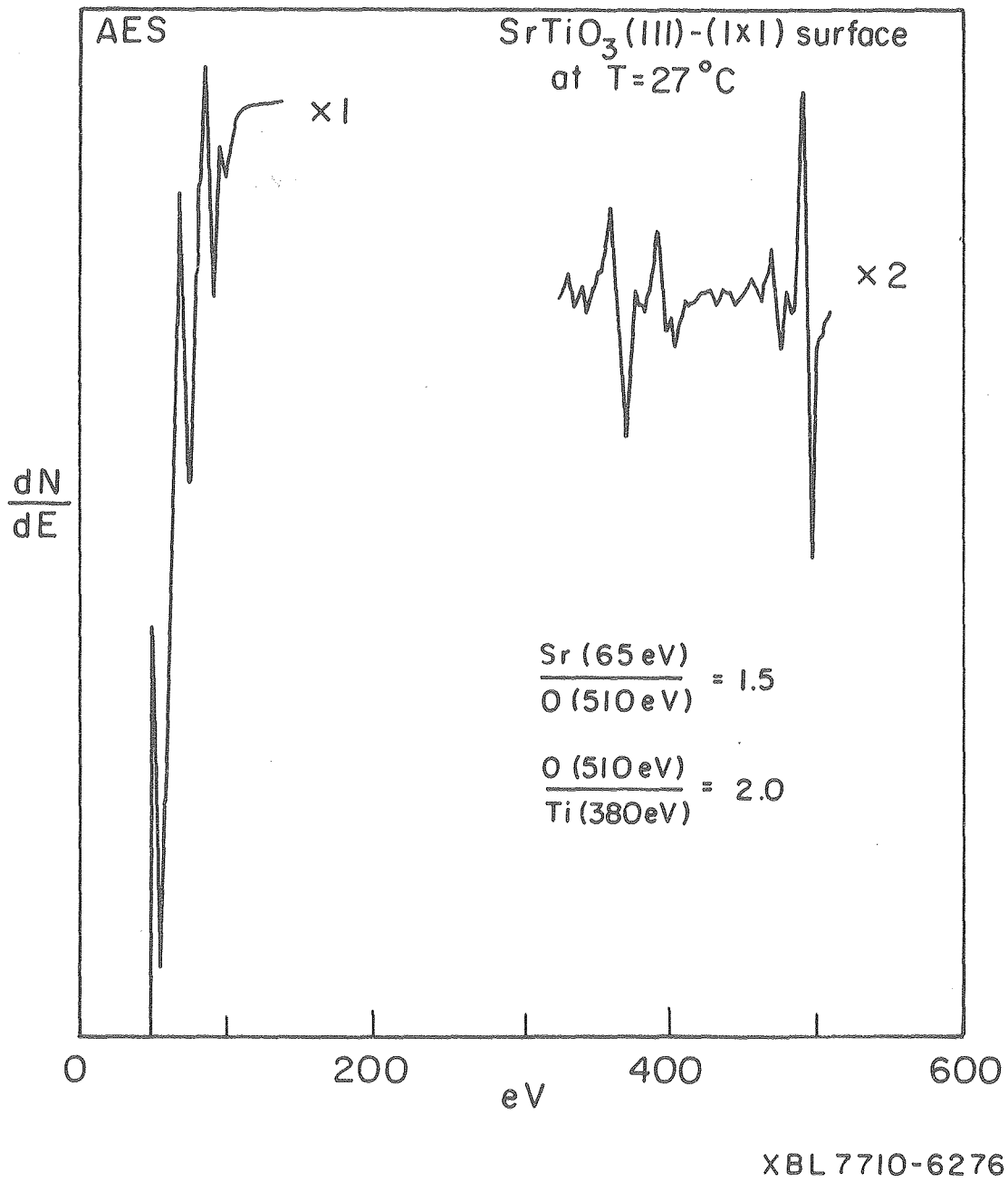

XBL 7710-6276

Fig. 3

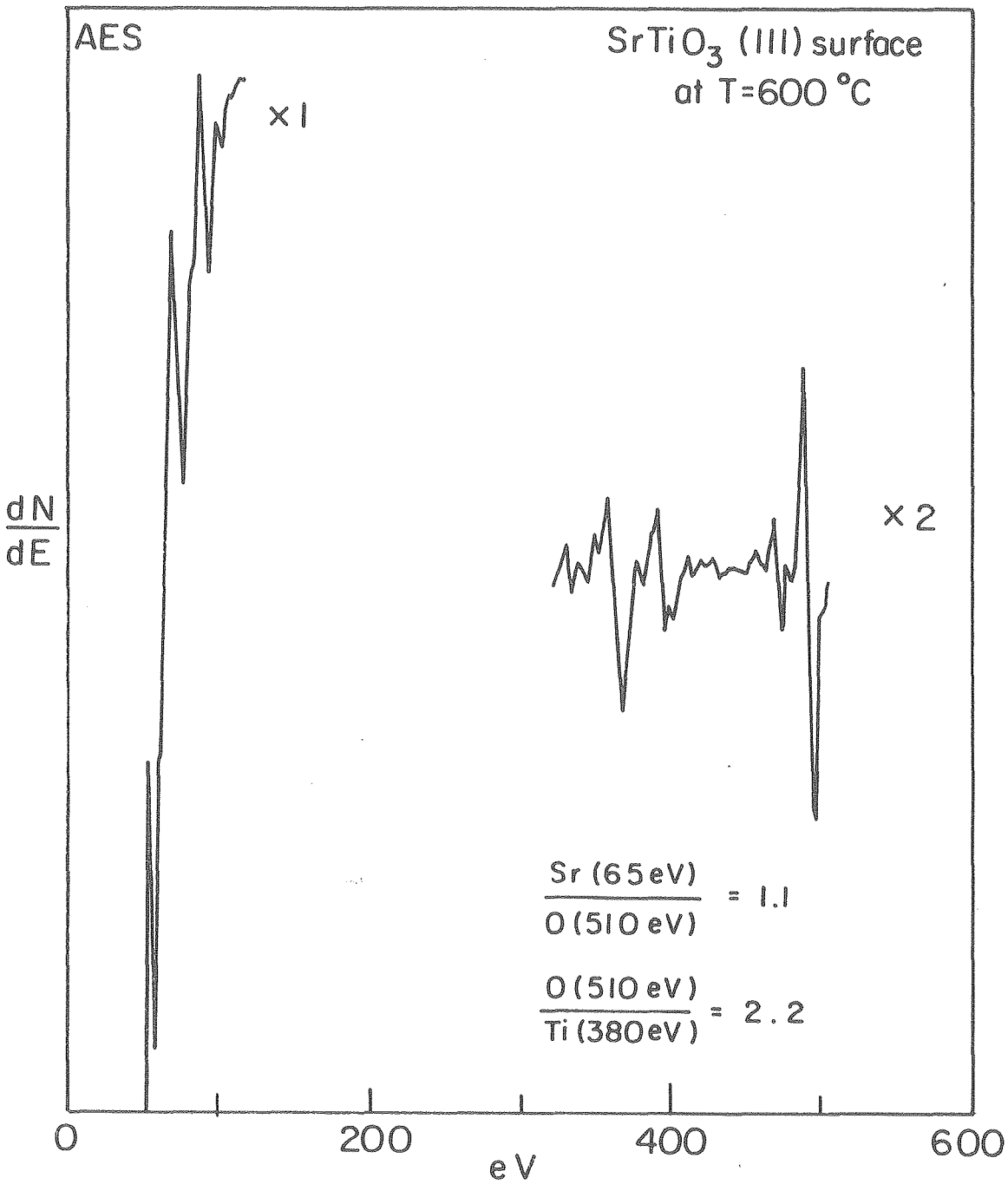

XBL 7710-6277

Fig. 4

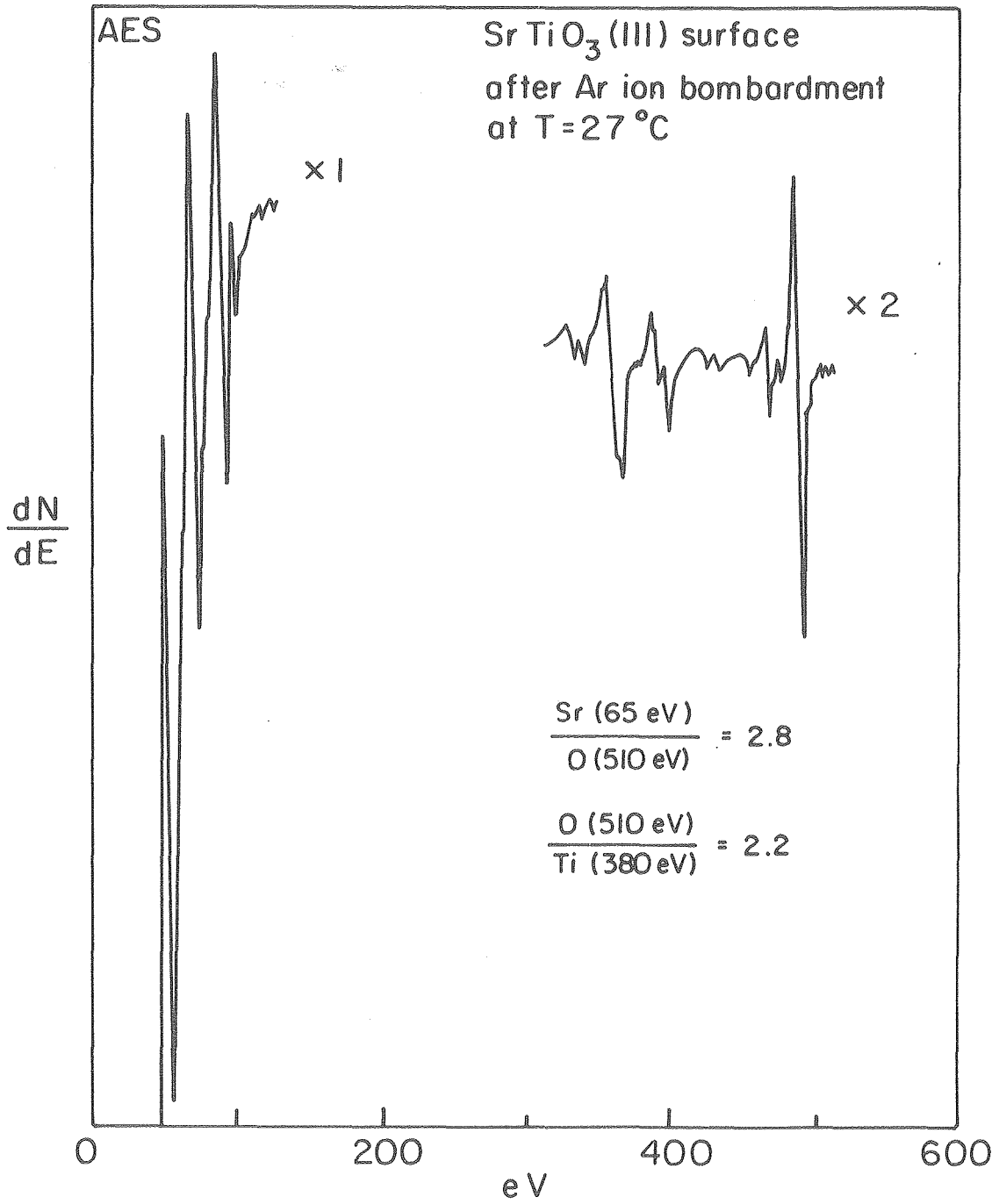

XBL 7710-6275

Fig. 5

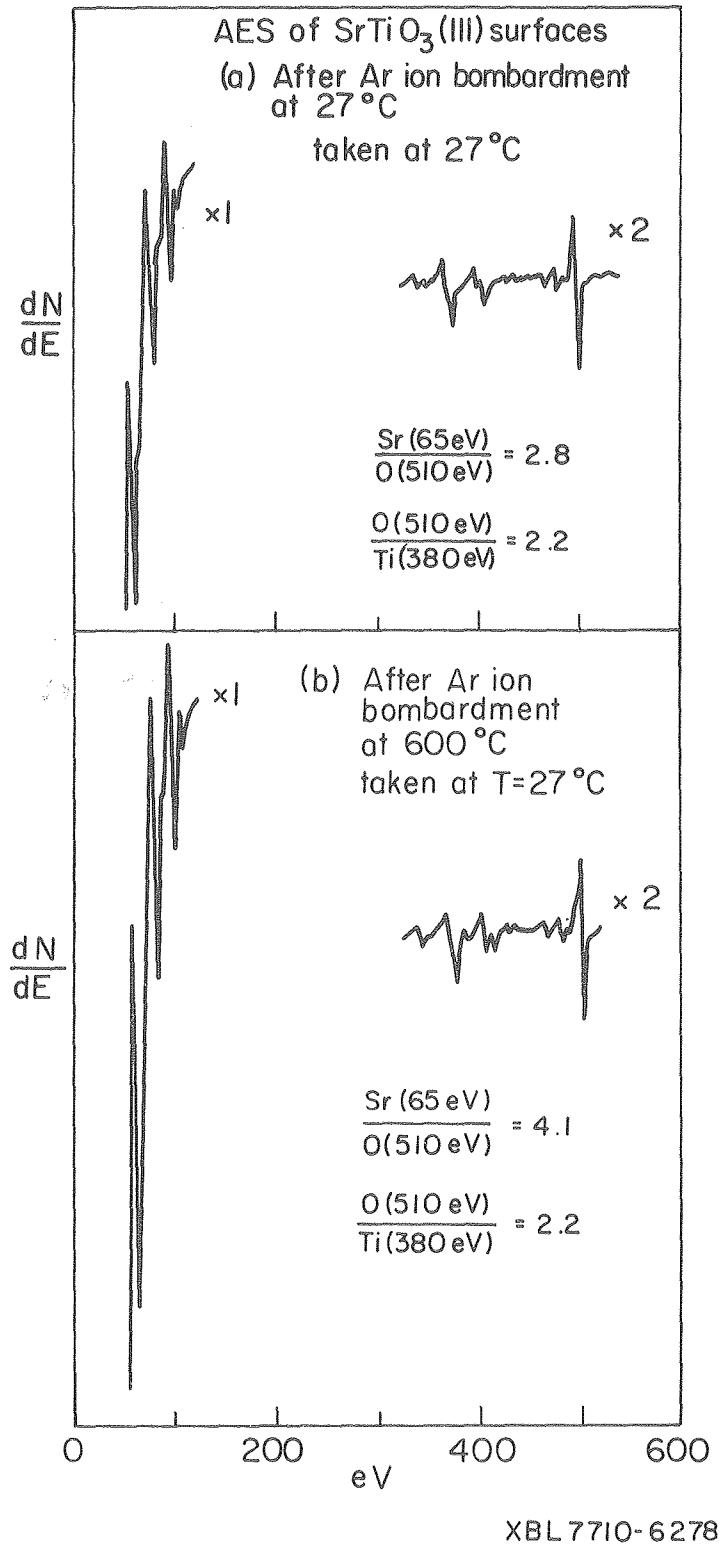

XBL 7710-6278

Fig. 6

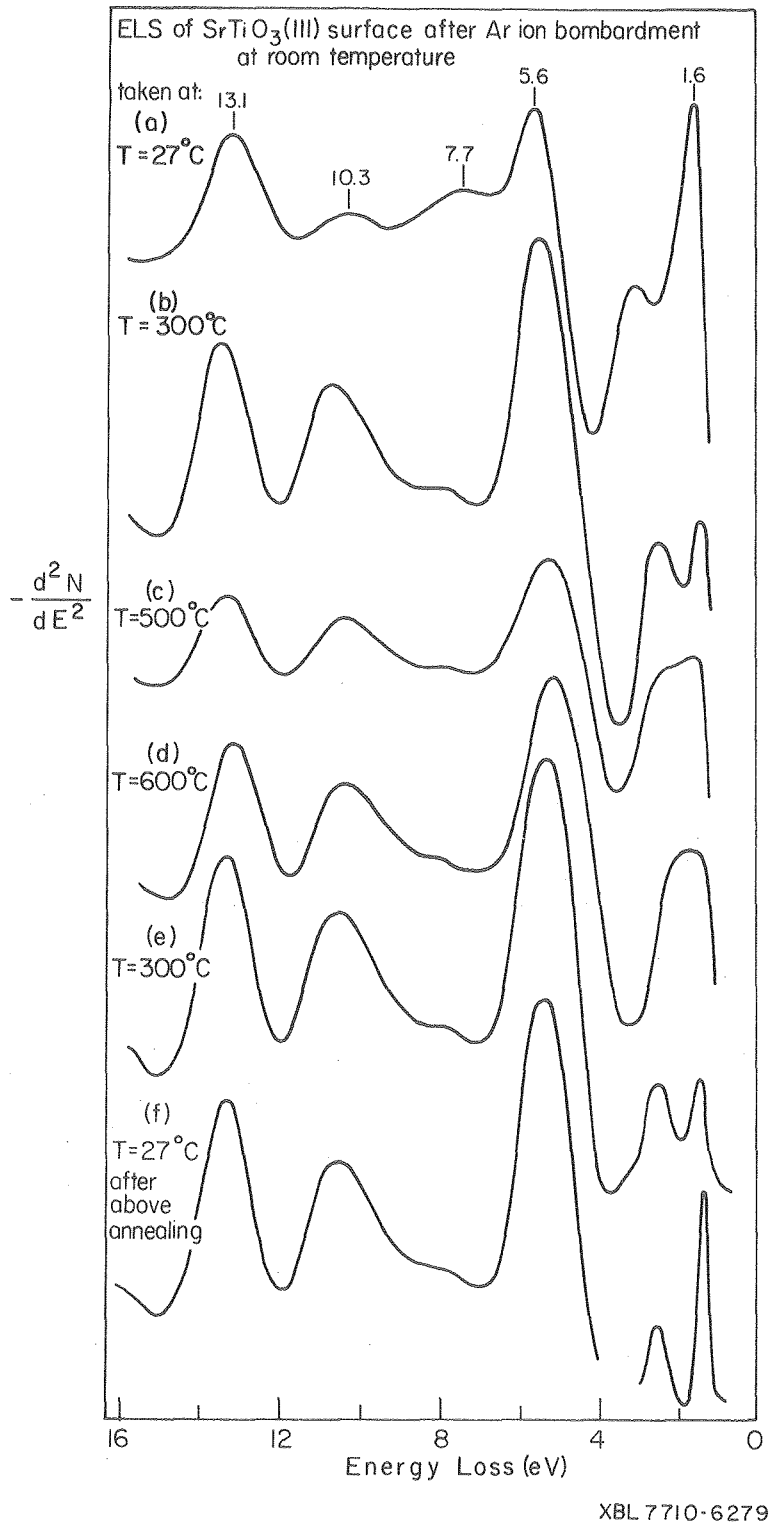
ELS of SrTiO3(111) surface after Ar ion bombardment
at room temperature
taken at:
(a)
T = 27°C
13.1
10.3
7.7
5.6
1.6
(b)
T = 300°C
(c)
T=500°C
(d)
T=600°C
(e)
T=300°C
(f)
T=27°C
after
above
annealing
$-\frac{d^2N}{dE^2}$
16
12
8
4
0
Energy Loss (eV)
XBL 7710-6279

Fig. 7

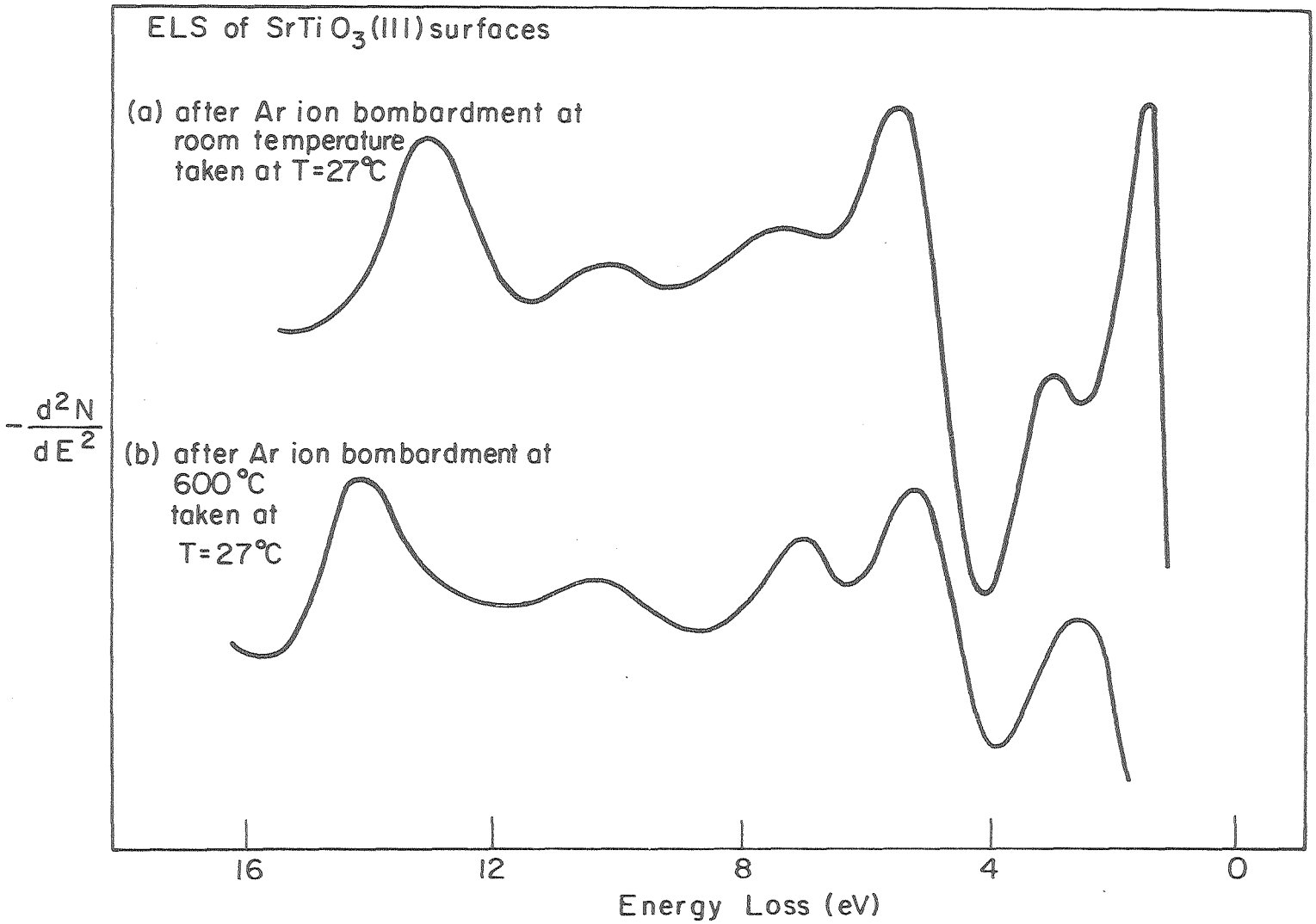

XBL 7710-6274

Fig. 8

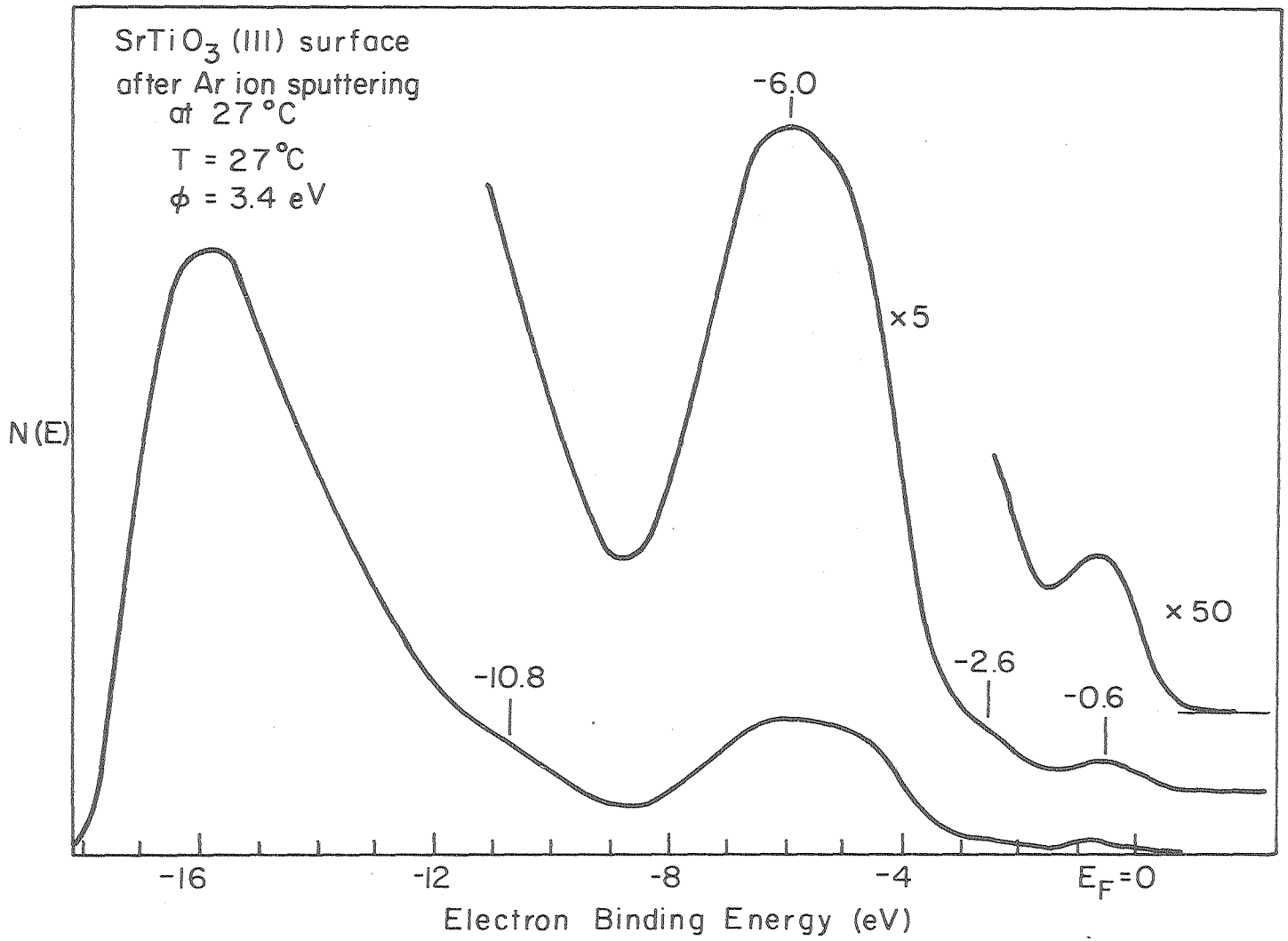

XBL 7710-6272

Fig. 9

0 0 0 0 4 9 0 3 7 2 0

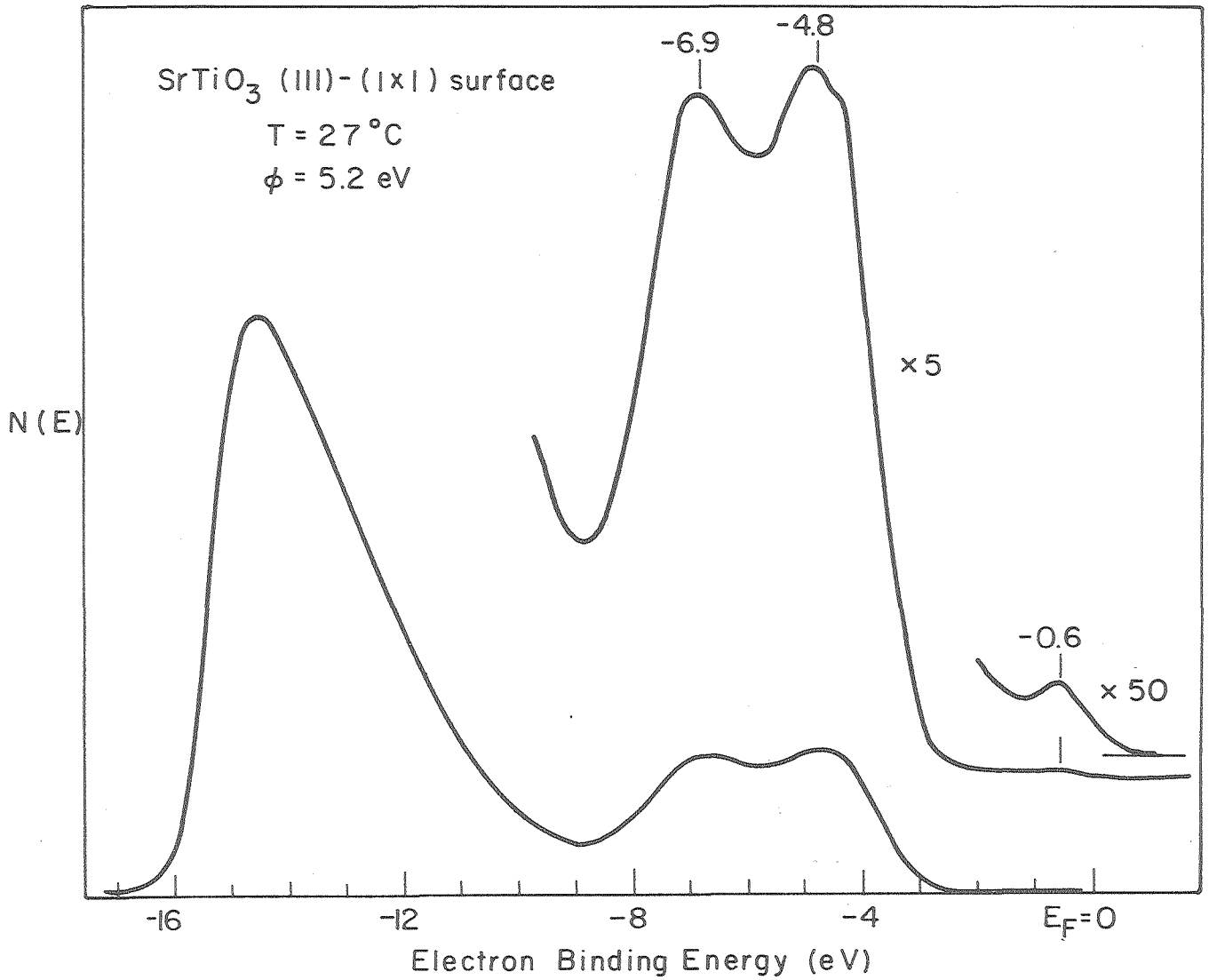

XBL 7710-6271

Fig. 10

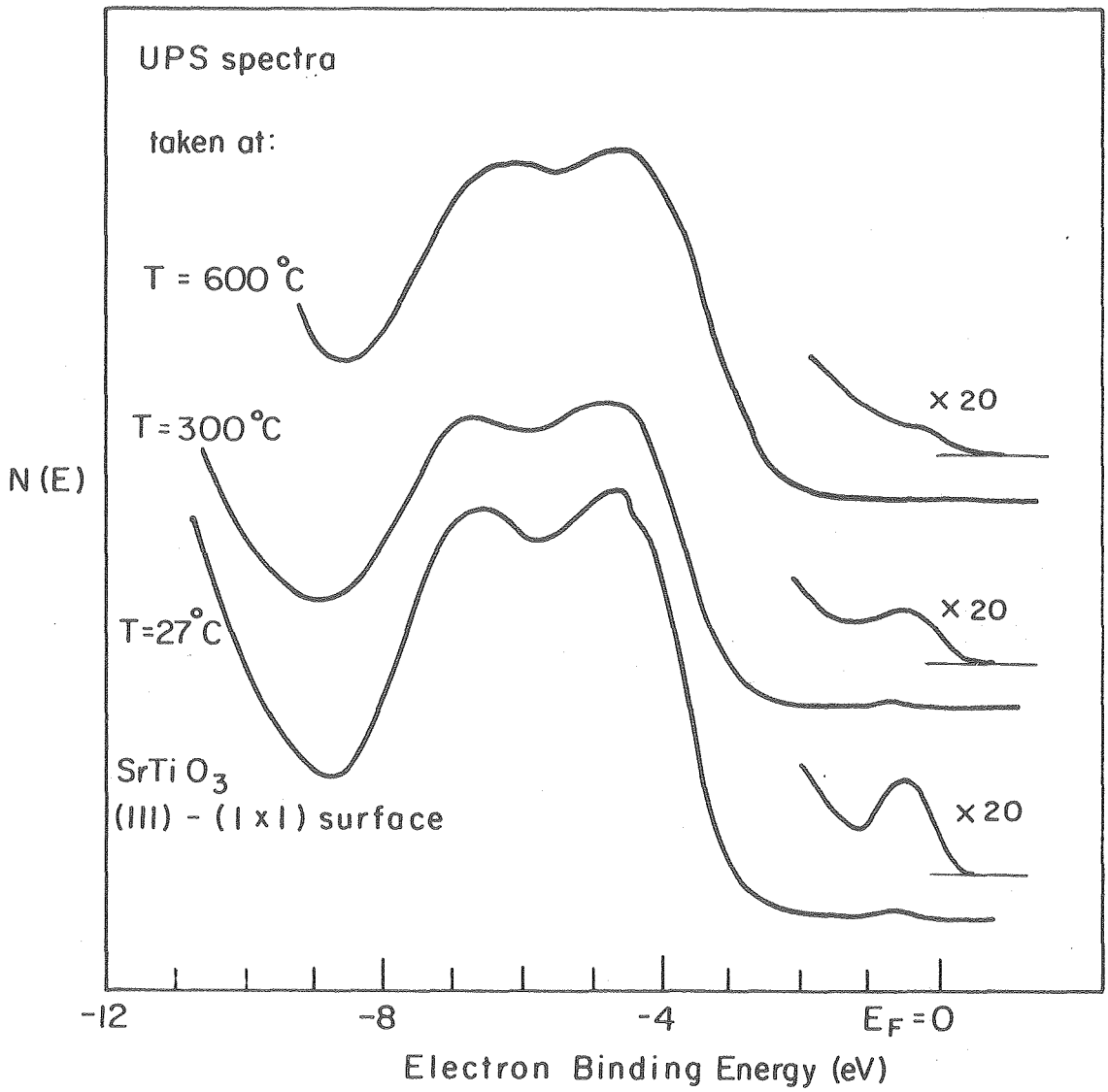

XBL 7710-6270

Fig. 11

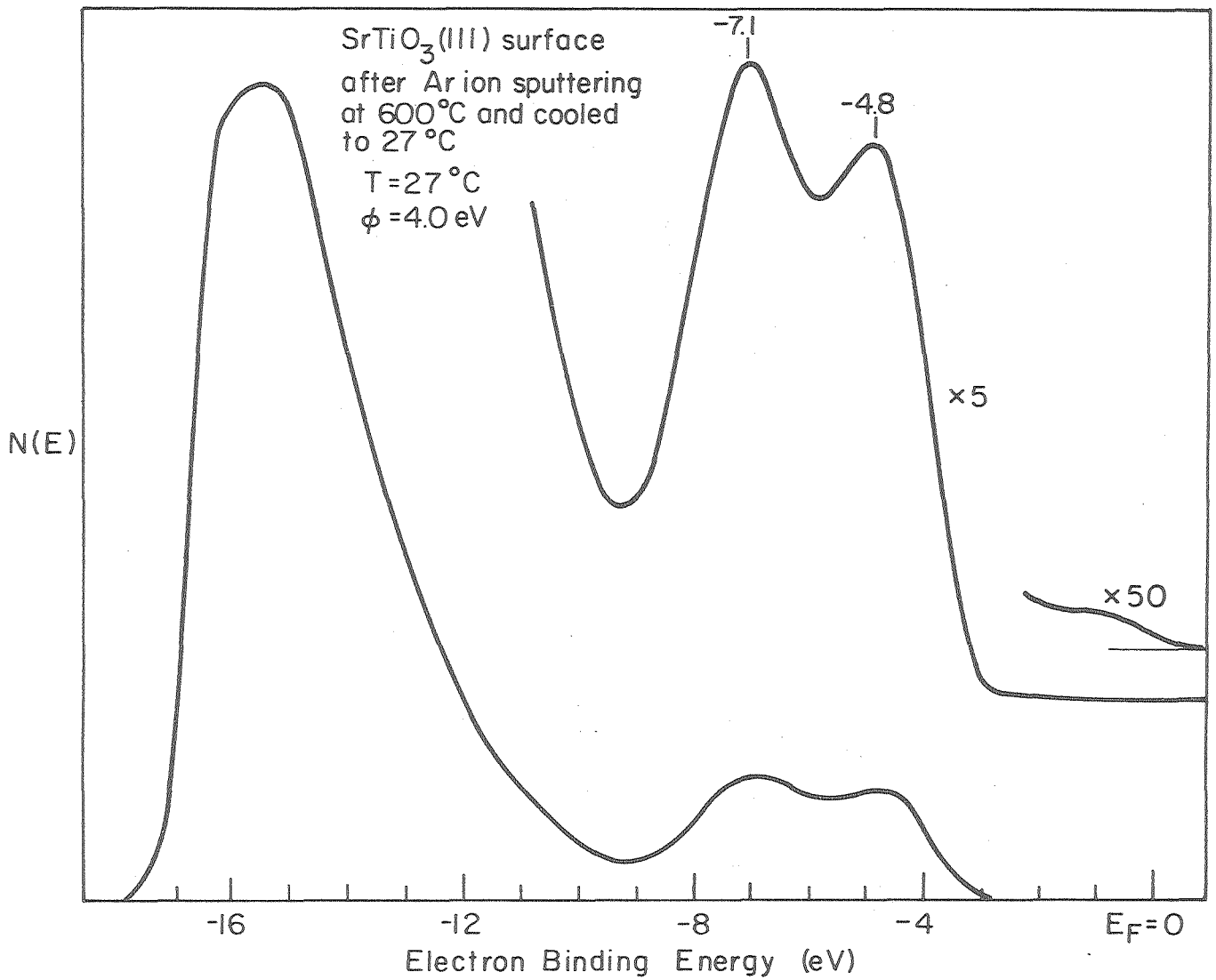

XBL7710-6273

Fig. 12

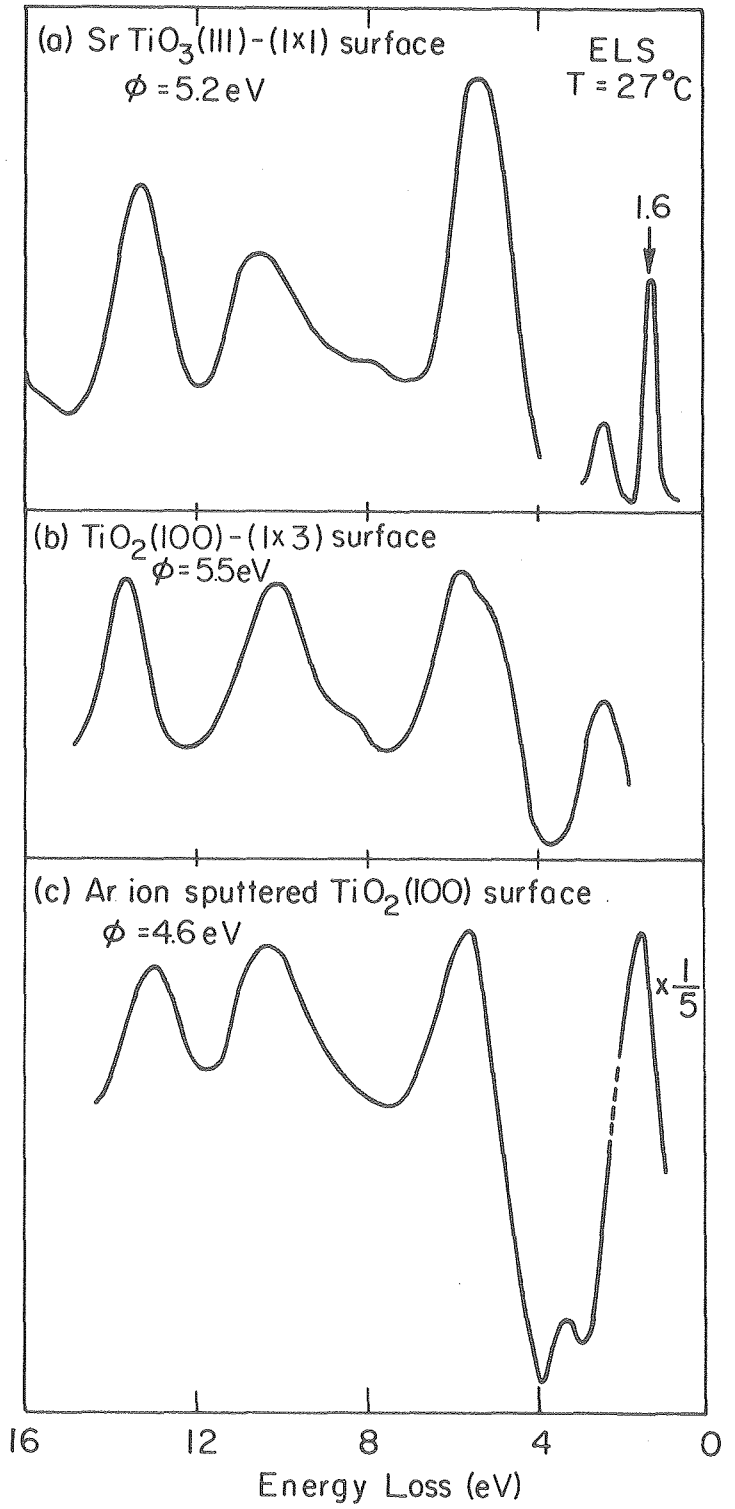

XBL 7711-6489

Fig. 13

This report was done with support from the United States Energy Research and Development Administration. Any conclusions or opinions expressed in this report represent solely those of the author(s) and not necessarily those of The Regents of the University of California, the Lawrence Berkeley Laboratory or the United States Energy Research and Development Administration.

0 0 0 0 4 5 0 2 2 9 4